

Molecular dynamics simulations of single-component bottle-brush polymers with a flexible backbone under poor solvent conditions

Nikolaos G Fytas¹ and Panagiotis E Theodorakis²

¹ Applied Mathematics Research Centre, Coventry University, Coventry, CV1 5FB, United Kingdom

² Department of Chemical Engineering, Imperial College London, London SW7 2AZ, United Kingdom

Abstract. Conformations of a single-component bottle-brush polymer with a fully flexible backbone under poor solvent conditions are studied by molecular-dynamics simulations, using a coarse-grained bead-spring model with side chains of up to $N = 40$ effective monomers. By variation of the solvent quality and the grafting density σ with which side chains are grafted onto the flexible backbone, we study for backbone lengths of up to $N_b = 100$ the crossover from the brush/coil regime to the dense collapsed state. At lower temperatures, where collapsed chains with a constant monomer density are observed, the choice of the above parameters does not play any role and it is the total number of monomers that defines the dimensions of the chains. Furthermore, bottle-brush polymers with longer side chains possess higher spherical symmetry compared to chains with lower side-chain lengths in contrast to what one may intuitively expect, as the stretching of the side chains is less important than the increase of their length. At higher temperatures, always below the Theta (Θ) temperature, coil-like configurations, similar to a single polymer chain, or brush-like configurations, similar to a homogeneous cylindrical bottle-brush polymer with a rigid backbone, are observed, depending on the choice of the particular parameters N and σ . In the crossover regime between the collapsed state (globule) and the coil/brush regime the acylindricity increases, whereas for temperatures outside of this range, bottle-brush polymers maintain a highly cylindrical symmetry in all configurational states.

PACS numbers: 02.70.Ns, 64.75.Jk, 82.35.Jk

Submitted to: *J. Phys.: Condens. Matter*

1. Introduction

Macromolecules with comb-like architectures, where linear or branched side chains [1] are grafted regularly or randomly onto a backbone chain have recently found much interest (for example, see the reviews [2, 3, 4, 5, 6, 7] and references therein). The interplay between steric repulsion of the side-chain monomers and effective attractive interactions that can be controlled by tuning the quality of the solvent, leads to intricate spatial self-organization of these molecular brushes. Such bottle-brush polymers can be either flexible or stiff, depending, not only on the chemical character of the backbone (which varies from a flexible macromolecule up to a stiff nanorod, e.g., a carbon nanotube [8, 9]), but, also, on the chain length N and the grafting density σ of the side chains. For example, by increasing N and σ , stiffening of intrinsically flexible backbones is induced, see, e.g., [3, 4, 10, 11, 12, 13, 14]. Moreover, conformations of such complex macromolecular objects can be sensitive to external stimuli (electric fields, light, or simply changes in the pH value of the solution). As a result, various relevant applications have been envisaged [2, 4]. In this work we do not follow this aspect; rather we focus our interest on the theoretical understanding of the structure formation of these molecular brushes by exploring the statistical mechanics of a coarse-grained model via molecular-dynamics (MD) simulations.

The study of the structure properties of bottle-brush polymers is a challenging task due to the multitude of length scales characterizing their structure [2, 10, 11, 12, 15]. However, computer simulations have been very useful to validate approximations needed to interpret experimental data [10, 12, 16, 17, 18, 19, 20, 21, 22, 23, 24, 25, 26]. Since some of the suggested applications require to consider bottle-brush polymers under poor solvent conditions, first steps to consider this case by theory [27] and simulations [28, 29, 30] have been taken. In particular, for bottle-brush polymers with a single type of side chains and rigid backbone, interesting *pearl-necklace* structures have been theoretically predicted [27] and validated by numerical simulations [29, 30]. These studies were also extended to bottle brushes with two different types of side chains grafted alternately onto the backbone [31, 32, 33], where such pearl-necklace structures were observed at intermediate grafting densities. On the other hand, Janus-type configurations were seen at high grafting densities. The main hypothesis of these works was that the backbone is strictly rigid falling in the case of a quasi-one-dimensional system, disregarding in this way any effect attributed to the flexibility of the backbone. The other extreme would be that the backbone is considered fully flexible, as the side chains of the brush. The latter case has only been studied for Θ and good solvent conditions by computer simulations [14, 34] and it was restricted to short chains, as the molecular weight in bottle brushes increases very fast with increasing the grafting density the backbone length and the length of the side chains. On the other hand, long chains are usually considered in theoretical work. As a result, a direct comparison with theoretical predictions is a delicate matter. In the present study, we consider for the first time the case of single-component bottle-brush polymers with a fully flexible

backbone under poor solvent conditions. By varying the grafting density, the solvent quality, and the backbone and side-chain length, we attempt to give a complete picture of the self-organization properties of such macromolecules in a poor solvent.

The rest of the paper is organized as follows: In the next section we give a brief theoretical background; in section 3, we present the model and the simulation methods. Then, section 4 defines and discusses the properties we monitor in our MD simulations. We close this manuscript in section 5, where we give a summary of our conclusions and an outline of future work.

2. Theoretical background

For bottle-brush polymers with a flexible backbone, no sharp phase boundaries [27] are expected to occur as it has been shown by MD simulations for bottle-brush polymers with a stiff backbone [29, 30]. Thus, we shall not describe any detailed calculations on how to derive phase boundaries here, but only give (background) qualitative arguments to understand the phenomena observed in our simulations. The cross-sectional linear dimension of a side chain of length N in the directions perpendicular to a rigid backbone and under good solvent conditions is expressed as a scaling relation [25, 27, 35, 36, 37, 38, 39, 40, 41, 42]

$$R_{cs} = N^\nu f(N^\nu \sigma) \rightarrow \sigma^{(1-\nu)/(1+\nu)} N^{2\nu/(1+\nu)}. \quad (1)$$

$\nu \approx 0.588$ is the characteristic exponent of a polymer chain under good solvent conditions [43], σ the grafting density, and f is a scaling function which describes the crossover from individual polymer *mushrooms* grafted onto the backbone of the bottle-brush with grafting density σ . As usually, pre-factors of order of unity are disregarded throughout. In this case, it has been shown [27, 33] that the densely grafted side chains are stretched in the radial directions. For individual polymer mushrooms the linear dimension R_z in the direction along the backbone also scales as $R_z \propto N^\nu$. Thus, the quantity $N^\nu \sigma$ defines the distance that neighboring side chains along the backbone start to interact, where the distance between grafting sites is σ^{-1} . Then, excluded volume interactions among the monomers of neighboring *mushrooms* start to cause chain stretching in radial direction. However, we should note here the power-law behavior $R_{cs} \propto N^{2\nu/(1+\nu)}$ can only be reached for very long chains, for which there also exists a significant regime where the radial monomer density profile decays with a related power law [25, 36, 37, 38, 39, 40, 41, 42]

$$\rho(r) \propto [r/\sigma]^{-(3\nu-1)/2\nu} \approx [r/\sigma]^{-0.65}, \quad \alpha \ll r \leq R_{cs}, \quad (2)$$

α being the distance between (effective) monomers along a side chain. As discussed in [25], for most cases of practical interest, one neither reaches the regime where equations (1) and (2) hold, nor are these equations suitable for chain lengths accessible to experiments [7].

Bottle-brush polymers under poor solvent conditions can be described with similar arguments to that of a collapsed polymer chain (see figure 1). For a solution near the Θ

temperature, scaling theories predict that the (gyration) radius R_c of the chain varies as [35]

$$R_c = N^{1/2}F(N^{1/2}\tau), \quad \tau = 1 - T/\Theta, \quad (3)$$

where the scaling function $F(Z)$ has the following limits:

$$\begin{aligned} F(Z \rightarrow \infty) &\propto Z^{-1/3}, \quad R_c \propto \tau^{-1/3}N^{1/3}, \quad \text{as } N \rightarrow \infty \\ F(Z = 0) &= \text{const.} \\ F(Z \rightarrow -\infty) &\propto Z^{2\nu-1}, \quad R_c \propto -\tau^{2\nu-1}N^\nu, \quad \text{as } N \rightarrow \infty. \end{aligned} \quad (4)$$

Here, $\nu = 0.588$ [43] is the well-known exponent [35], and the limits $N \rightarrow \infty$ and $\tau \rightarrow 0$ are such that $|Z| \leq \infty$. As usually done, we ignore both logarithmic corrections, that are expected to occur at the Θ point [44, 45], and corrections to scaling that actually do become important for not very large N [14].

One may often attempt to interpret scaling theories as a comparison of lengths [35]. The size of a polymer coil in a Θ solvent is described by the scaling law $R_c = \alpha N^{1/2}$, where α is the size of the monomeric unit. Thus, the relation $Z = N^{1/2}\tau$ can also be written as $Z = R_c/\xi$, $\xi = \alpha/\tau$, where the latter is the size of a *thermal blob* [35, 46, 47]. For collapsed globules, slightly below the Θ point [equation (4)], the structure of the coil can be described as a dense packing of blobs, each one of size $\xi = \sqrt{n}\alpha$, where n is the number of monomers per blob. Then, the number of these blobs is $n_b = N/n = N/(\xi/\alpha)^2$. The density inside this coil should be essentially constant (figure 2) and is described by the following equation

$$\rho = n/\xi^3 = 1/(\alpha^2\xi) = \tau/\alpha^3. \quad (5)$$

The surface region of the globule is just the outer shell of the blobs, of thickness ξ , giving rise to a surface free energy (surface tension) $\gamma = n_b^s/R_c^2$, $n_b^s = n_b^{2/3}$ being the number of blobs in this outer shell (remember that the free-energy cost of one blob is $k_B T$). Using equation (4) and omitting all geometric pre-factors one end with

$$\gamma = \left(\frac{n_b}{R_c^3}\right)^{2/3} = \tau^2\alpha^{-2}. \quad (6)$$

Equations (5) and (6) characterize isolated free chains and individually collapsed side chains onto the rigid backbone of a bottle-brush, as long as the $h = \sigma^{-1}$ is large enough, so that there is no free-energy gain when neighboring collapsed globules coalesce. Such relations can also describe bottle-brush polymers with a flexible backbone in the collapsed state (see figure 2). Thus, the total surface free energy of a collapsed bottle-brush polymer with a flexible backbone is of the order of $R_c^2\gamma = N^{2/3}\tau^{4/3} = (N\tau^2)^{2/3}$.

For rigid backbones, when the distance h and the radius R_c of the collapsed chain [as described by equation (4)] become comparable, the system can minimize its free-energy cost if two, or more neighboring globular chains, coalesce [27, 29, 30, 33]. If we assume that the number of thermal blobs remains constant, the bulk free energy decides on the stability of the different structures. The object formed by coalescence of two collapsed coils that are grafted at a distance h , clearly will result in an elongated object of length

L along the backbone and radius R in the plane perpendicular to the backbone, with $R \leq L$. The formation of such structures results in a free-energy penalty of the order of τ [27, 47]. Thus, the free-energy cost of a cluster formed by m neighboring chains grafted within a distance $L = mh$ is [27]

$$\Delta F_1(m)/k_B T = (mN\tau^2)^{2/3} - m(N\tau^2)^{2/3} + m^2(h/\alpha)\tau. \quad (7)$$

The total number of monomers in a cluster formed from m chains is mN , and hence the total surface free-energy cost of such an object is $(mN\tau^2)^{2/3}$, whereas the total surface free-energy cost of m separated globules, that contain N monomers each, is $m(N\tau^2)^{2/3}$. The last term $m^2 h \tau$ is the total elastic stretching energy and scales quadratically in m , as expected. Such an analysis is relevant for bottle brushes with a rigid backbone, whereas for bottle-brush polymers with a flexible backbone, only two regimes of rather homogenous structures occur (see figure 1): the collapsed chain state for temperatures further from the Θ regime, and the coil/brush regime, for temperatures close to the Θ temperature. Therefore, *pearl-necklace*-like structures are fully attributed to the backbone stiffness [29].

3. Model and simulation methods

For bottle-brush polymers with flexible backbones under poor solvent conditions [29, 30] we describe both the backbone chain and the side chains by a bead-spring model [48, 49, 50], where all beads interact with a truncated and shifted Lennard-Jones (LJ) potential $U_{\text{LJ}}(r)$ and nearest neighbors, bonded together along a chain, also experience the finitely extensible nonlinear elastic (FENE) potential $U_{\text{FENE}}(r)$, r being the distance between the beads. Thus,

$$U_{\text{LJ}}(r) = 4\epsilon_{\text{LJ}} \left[\left(\frac{\sigma_{\text{LJ}}}{r} \right)^{12} - \left(\frac{\sigma_{\text{LJ}}}{r} \right)^6 \right] + C, \quad r \leq r_c, \quad (8)$$

while $U_{\text{LJ}}(r > r_c) = 0$, and $r_c = 2.5\sigma_{\text{LJ}}$. The constant C is defined such that $U_{\text{LJ}}(r = r_c) = 0$ is continuous at the cut-off. Henceforth, units are chosen such that $\epsilon_{\text{LJ}} = 1$, $\sigma_{\text{LJ}} = 1$, the Boltzmann constant $k_B = 1$, and also the mass m_{LJ} of all beads is chosen to be unity. The potential of equation (8) acts between any pair of beads, irrespective of whether they are bonded or not. For bonded beads also the potential $U_{\text{FENE}}(r)$ acts, where

$$U_{\text{FENE}}(r) = -\frac{1}{2}kr_0^2 \ln \left[1 - \left(\frac{r}{r_0} \right)^2 \right] \quad 0 < r \leq r_0, \quad (9)$$

$r_0 = 1.5$, $k = 30$, and $U_{\text{FENE}}(r) = \infty$ outside the range written in equation (9). Hence r_0 is the maximal distance that bonded beads can take. Note that we did not include any explicit solvent particles; solvent-mediated interactions and solvent quality are only indirectly simulated by varying the temperature of the system.

In our model there is no difference in interactions, irrespective of whether the considered beads are effective monomers of the backbone or side chains. This implies that, the polymer forming the backbone is either chemically identical to the polymers

that are tethered as side chains to the backbone, or at least on coarse-grained length scales, as considered here, the backbone and side chain polymers are no longer distinct. There is also no difference between the bond linking the first monomer of a side chain to a monomer of the backbone and bonds between any other pairs of bonded monomers. Of course, our study does not address any effects due to a particular chemistry relating to the synthesis of these bottle-brush polymers, but, as usually done [50], we address universal features of the conformational properties of these macromolecules.

There is one important distinction comparing to our previous work [29] on bottle-brush polymers with rigid backbones: in [29] the backbone was taken, following Murat and Grest [49], as an infinitely thin straight line in continuous space, thus allowing arbitrary values of the distances between neighboring grafting sites, and hence the grafting density σ could be continuously varied. For the present model, where we disregard any possible quenched disorder resulting from the grafting process, of course, the grafting density σ is quantized: we denote here by $\sigma = 1.0$ the case that every backbone monomer carries a side chain, $\sigma = 0.5$ means that every second backbone monomer has a side chain, etc. Chain lengths of side chains were chosen as $N = 4, 10, 20$, and $N = 40$, while backbone chain lengths were chosen as $N_b = 50$ and $N_b = 100$, respectively. It is obvious that for such short side-chain lengths and under poor solvent conditions any interpretation of characteristic lengths is a delicate matter for specified range of rather small values of N . However, we should emphasize that our range of N nicely corresponds to the range available in experiments [2, 4, 10, 11, 12, 51] and that the simulation of longer chains becomes an extremely cumbersome task, as relaxation times are increasing exponentially. Already for bottle-brush polymers under Θ and good solvent conditions equilibration of bottle-brush polymers with long backbones [14] (e.g., $N_b = 200$) required an enormous effort. We do not attempt to reach such backbone lengths here.

Unfortunately, for the model defined in equations (8) and (9), the Θ temperature is known only rather roughly [52], namely, $\Theta \approx 3.0$. Being interested in $T \leq \Theta$, we have attempted to study the temperature range $1.5 \leq T \leq 3.0$. Note however that, equilibration of collapsed chains is rather difficult, as will be discussed below, besides the particular problems encountered due to the multitude of length scales in a bottle-brush macromolecule. In our simulations, the temperature is controlled by the Langevin thermostat, following previous work [50, 53, 54, 55, 56, 57]. The equation of motion for the coordinates $\{r_i(t)\}$ of the beads

$$m \frac{d^2 \mathbf{r}_i}{dt^2} = -\nabla U_i - \gamma \frac{d\mathbf{r}_i}{dt} + \Gamma_i(t) \quad (10)$$

is numerically integrated using the GROMACS package [58, 59]. In equation (10), t denotes the time, U_i is the total potential acting on the i -th bead, γ is the friction coefficient, and $\Gamma_i(t)$ is the random force. As it is well-known, γ and Γ are related via the usual fluctuation-dissipation relation

$$\langle \Gamma_i(t) \cdot \Gamma_j(t') \rangle = 6k_B T \gamma \delta_{ij} \delta(t - t') \quad (11)$$

Following references [50, 52, 57], the friction coefficient was chosen as $\gamma = 0.5$. Equation (10) was integrated with the leap-frog algorithm [60] using an integration time step of $\Delta t = 0.006\tau$, where the MD time unit is $\tau = (m_{\text{LJ}}\sigma_{\text{LJ}}^2/\epsilon_{\text{LJ}})^{1/2} = 1$.

Firstly, the system was equilibrated at a temperature $T = 3.0$ using simulations extending over a time range of $30 \times 10^6\tau$. To gather proper statistics, we used 500 independent configurations at this high temperature, as initial configurations for slow cooling runs, where the temperature was lowered in steps of 0.1, and the system was simulated, at each temperature, for a time of $5 \times 10^6\tau$. The final configuration of each (higher) temperature was used as starting configuration for the next (lower) temperature. In this way, one can safely generate, at low temperatures and intermediate values of grafting densities, statistically independent configurations. Let us point out here that, standard MD simulations would typically not sample phase space adequately at this low-temperature regime. However, this problem was surpassed here by carrying out this large number of independent slow cooling runs (typically around 500 runs). The statistical accuracy of our results was also checked by varying on the same footing the cooling speed and length of runs. For temperatures above $T = 2.0$ correlations are rather insignificant, but for temperatures below $T = 2.0$ this slow cooling methodology is indispensable in order to get reliable results for our chosen range of parameters.

4. Results

In the case of a single-component bottle-brush polymer with a strictly rigid backbone and at low grafting densities, side chains collapse individually onto the backbone. When the grafting density, or the side-chain length increases, chains start forming clusters which consist of more than one side chain. Further increase of the grafting density (or very long side chains) to the so-called *brush* regime, leads to an homogeneously cylindrical structure [29, 30]. When we study the case of a single-component bottle-brush polymer with a fully flexible backbone under poor solvent conditions, we can basically distinguish two regimes: At low temperatures, or poor solvent conditions, relatively far from the Θ point, the chain obtains an almost spherical structure, like those in the left part of figure 1 for either lower or higher grafting density, shorter or longer backbone, and shorter or longer side chains (we shall discuss the shape of this spherical form later in this section). On the other hand, at temperatures close to the Θ temperature, gaussian-like chains are formed for very low grafting density and short side chains or almost homogenous cylindrical brushes as the grafting density and side-chain length increase, as clearly shown in the right part of the same figure.

The first quantity we have computed is the overall monomer density, mathematically expressed by the following formula

$$\rho(|\vec{r}|) = \left\langle \sum_{i=1}^{nN} \delta(\vec{r} - \vec{r}_c - \vec{r}_i) \right\rangle, \quad (12)$$

where $\delta(\vec{x})$ is the Dirac delta function, \vec{r}_c the position of the center of mass of all monomers that belong to the chain, and \vec{r}_i the positions of all monomers, irrespective

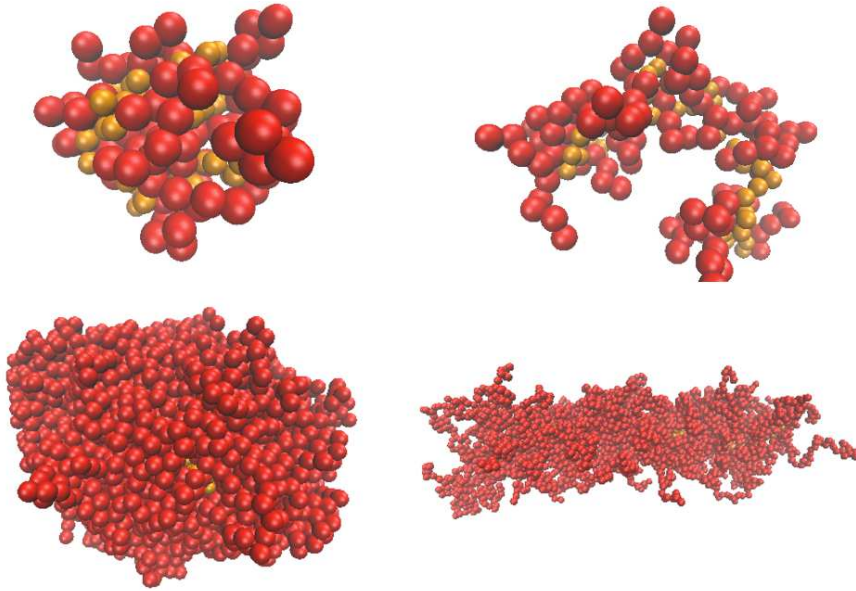


Figure 1. (Color online) Characteristic snapshots of bottle-brush polymers with a flexible backbone. In the left part snapshots are taken at temperature $T = 1.5$, whereas on the right part at $T = 3.0$. Upper part refers to a bottle-brush with parameters $\sigma = 0.5$, $N_b = 50$, and $N = 5$, whereas in the lower part we consider $\sigma = 1.0$, $N_b = 100$, $N = 40$. At low temperatures, chains are in the collapsed state (globule), similar to a single polymer chain, whereas at the higher temperature we distinguish between a coil-like structure and an almost homogeneous cylindrical brush similar to a homogeneous cylindrical brush with a rigid backbone.

of whether they belong to the backbone or not. The angle brackets denote an average over all conformations, as usual. Figure 2 shows two characteristic examples of the overall monomer density. At temperature $T = 1.5$, it is clear that the bottle-brush polymer, close to its center of mass, has a constant density near to the melt polymer density, as expected. Then, the density profile decays far from its center of mass and the starting point of this decay depends only on the total number of beads of the bottle-brush macromolecule. Therefore, any effects attributed to the specific architecture of bottle-brush polymers are not coming onto the surface at such low temperatures. We will later see what is the range of temperature that corresponds to the collapsed state. Furthermore, this density decay does not reveal any significant behavior that could be attributed to the specific macromolecular architecture. On the other hand, the effect of architecture is more noticeable at temperatures close to the Θ temperature, where the increase of the grafting density σ and the chain length N results in a more extended density profile with distance r . Furthermore, the gradual lowering of the temperature from the brush regime to the collapsed chain regime (inset of figure 2) does not hint for any sharp transition; we observe a smooth variation of the density profile as the

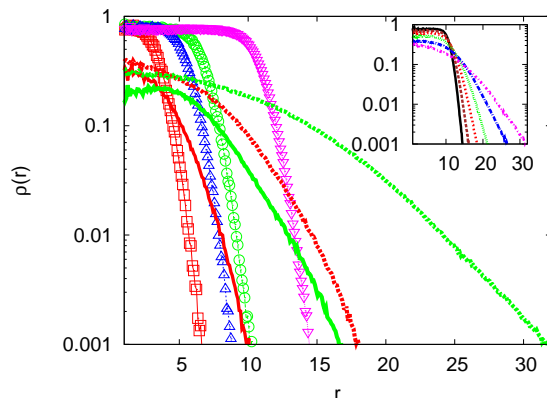


Figure 2. (Color online) Density profiles as a function of the distance from the center of mass of a bottle-brush at $T = 1.5$ (open symbols) and $T = 3.0$ (lines). Squares or continuous red line refer to $\sigma = 0.5$, $N_b = 50$, and $N = 5$, circles or the dashed red line to $\sigma = 0.5$, $N_b = 50$, and $N = 40$, triangles or the continuous green line to $\sigma = 1.0$, $N_b = 100$, and $N = 5$, and upside-down triangles or the dashed green line to $\sigma = 1.0$, $N_b = 100$, and $N = 40$. The inset illustrates the density profile for the case $\sigma = 1.0$, $N_b = 100$, and $N = 40$ as a function of temperature. The continuous black line corresponds to $T = 1.5$ and temperatures up to $T = 3.0$ are shown with step $\Delta T = 0.3$. No signs of sharp phase transition between the collapsed state and the brush regime are observed.

temperature is decreased. The same behavior is observed for all the bottle brushes of this study.

Following the definition of standard textbooks, aspects related to the persistence length of the polymer chains may be discussed, where the persistence length is defined from the decay of bond orientational correlations along the chain [14]. However, one should be careful when attempts to estimate the persistence length of polymer chains, as for solvent conditions other than Θ , different definitions account for different values of the persistent length [14]. Defining the bond vectors $\vec{\alpha}_i$ in terms of the monomer positions \vec{r}_i as $\vec{\alpha}_i = \vec{r}_{i+1} - \vec{r}_i$, $i = 1, \dots, nN - 1$, the bond orientational correlation is given by

$$\langle \cos\Theta(s) \rangle = l_b^{-2} \frac{1}{N_b - 1 - s} \sum_{i=1}^{N_b-1-s} \langle \vec{\alpha}_i \cdot \vec{\alpha}_{i+s} \rangle. \quad (13)$$

Note that $\vec{\alpha}_i^2 = l_b^2$, with l_b being the average bond length. For this model $l_b \approx 1$ and hence $\langle \cos\Theta(0) \rangle \approx 1$. Considering the limit $nN \rightarrow \infty$ and assuming Gaussian chain statistics, one obtains an exponential decay, since then $\langle \cos\Theta(s) \rangle = \langle \cos\Theta(1) \rangle^s = \exp[s \ln \langle \cos\Theta(1) \rangle]$, and thus

$$\langle \cos\Theta(s) \rangle = \exp[-s/l_p], \quad l_p^{-1} = -\ln \langle \cos\Theta(1) \rangle. \quad (14)$$

For chains at the Θ point [61] or in melts [62] one has

$$\langle \cos\Theta(s) \rangle \propto s^{-3/2}, \quad s \rightarrow \infty. \quad (15)$$

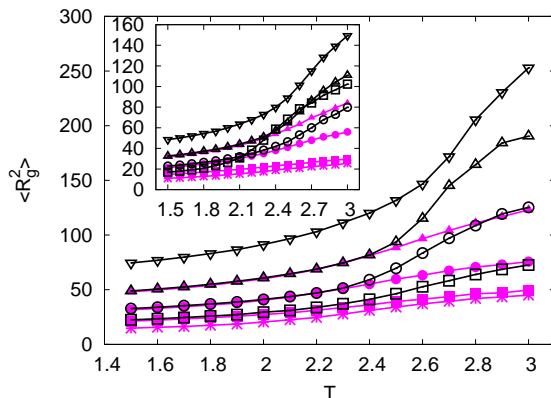


Figure 3. (Color online) Mean-square gyration radius for the whole bottle-brush polymer as a function of the temperature. In the main part data refer to $\sigma = 1.0$, whereas the inset illustrates data for $\sigma = 0.5$. Full symbols correspond to $N_b = 50$ and open symbols to $N_b = 100$ for both grafting densities. Curves correspond to $N = 5, 10, 20$, and $N = 40$, starting from the bottom.

By measuring this property we have verified that in the collapsed states of figure 1 correlations along the backbone die out very quickly and within the range of 2 – 4 monomers, depending on the choice of parameters. Of course, for the case $\sigma = 1.0$ and $N = 40$ some more correlation is observed, which, however, does not justify any further analysis of these data. Also, we were not able to detect any kind of correlation patterns similarly to the case of multi-block copolymers in a poor solvent [56].

Turning back our discussion to the properties related to the size of the bottle-brush polymers, we calculated properties such as the mean-square gyration radius of the whole bottle brush $\langle R_g^2 \rangle$, backbone $\langle R_{g,b}^2 \rangle$, and side chains $\langle R_{g,s}^2 \rangle$, as well the end-to-end distance of the backbone $\langle R_{e,b}^2 \rangle$. Figure 3 presents results for the mean-square gyration radius of the whole macromolecule, as a function of the temperature. This property confirms our conclusions from figure 2 that bottle brushes with the same number of monomers at low temperatures have the same dimensions in the collapsed state, achieving a constant density close to the center of mass and a similarly decay pattern far from the center. This behavior persists over a higher range of temperatures, as the total number of monomers increases, and provides a rough estimation of the onset of the collapsed state as the temperature is lowered. This behavior is seen at both $\sigma = 0.5$ and 1.0 cases.

On the other hand, $\langle R_{g,s}^2 \rangle$ exhibits a dependence on the particular parameters of the bottle brush for the whole range of temperatures, below the Θ temperature (we refer to figure 4). However, it is a subtle issue to make any quantitative statement, as our analysis is restricted to short side-chain lengths. Qualitatively, one may note that the side chains and the backbone rearrange themselves in such a way at low temperatures, that the overall density close to the center of mass remains constant. This is what is seen if one combines the data of figures 4 and 5. Furthermore, by plotting the data

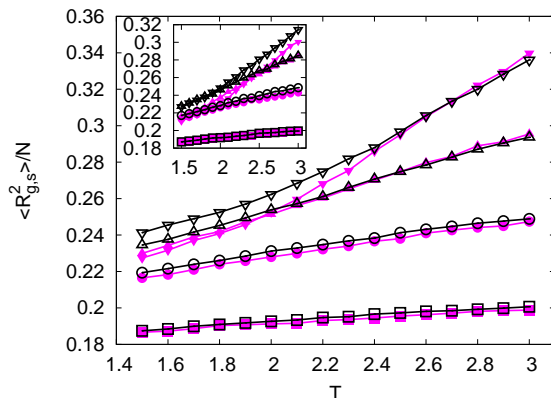


Figure 4. (Color online) Mean-square gyration radius of the side chains divided by the side-chain length N as a function of temperature for different cases. Symbols are chosen in the same way as in figure 3.

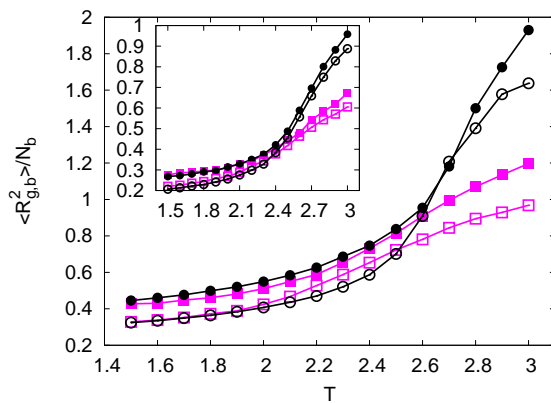


Figure 5. (Color online) Mean-square gyration radius of the bottle-brush backbone normalized by the backbone chain length N_b as a function of the temperature for $N = 40$ (full symbols) and $N = 20$ (open symbols). We consider $\sigma = 1.0$ (main panel) and $\sigma = 0.5$ (inset). Black lines and symbols correspond to $N_b = 100$, whereas the corresponding magenta colored lines and symbols to $N_b = 50$.

for different chain lengths, such as the data of figure 5 for the backbone dimensions normalized with N_b , we get an estimate for an “effective” Θ temperature of the backbone. Apparently, the Θ temperature of the model for a single polymer chain is different to that of the bottle-brush backbone due to the presence of the side chains, which introduce an overall stiffness on the macromolecule. For $N = 20$ this crossing of the curves for $N_b = 50$ and $N_b = 100$, may suggest a Θ temperature while keeping constant σ and N . On the other hand, as N increases to 40, we obtain a behavior that is similar to the case of a cylindrical bottle-brush with a rigid backbone [29]. That is an overlap of the curves at low enough temperatures. A detailed discussion about this feature can be found in [29]. It would be also interesting to obtain data for longer backbones, but this is an enormously difficult task for bottle-brush macromolecules under poor solvent conditions.

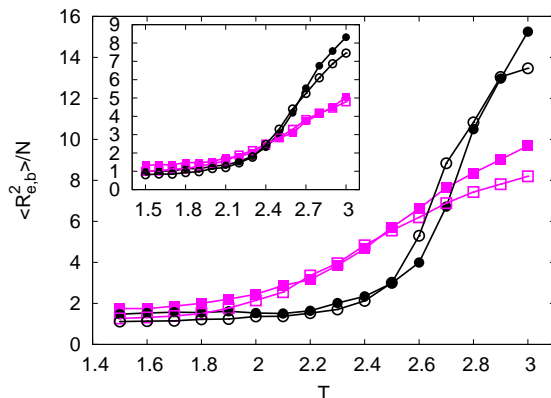


Figure 6. (Color online) Same as in figure 5, but the end-to-end distance of the bottle-brush backbone is plotted as a function of the temperature.

Already under Θ and good solvent conditions equilibration of such macromolecules with long backbones has been proven extremely challenging (e.g., $N_b = 200$) due to the existence of the so-called *breathing modes* [14]. Measuring the end-to-end distance of the bottle-brush backbone, figure 6, reveals similar effects, but this quantity is more reliable when one makes a comparison with the theoretical predictions. Although our study is limited by the chain lengths, we do not expect any qualitatively different behavior in the long-chain limit.

Figure 7 presents results for the mean-square gyration radius of the side chains as a function of the chain length N . Whereas for higher temperatures one can observe the onset of a scaling regime with N , as expected (see also [14]), at lower temperatures, and $N > 20$, there is only a weak dependence on the side-chain length N . This is an indication that also the side chains themselves exhibit a constant density regime close to their center of mass, similarly to the case of the whole bottle-brush macromolecule. It is rather naive and misleading to discuss any attempts of scaling, but we have found good agreement with $N^{1/3}$, for our backbones of the bottle-brush macromolecule.

An interesting aspect of our discussion is based on the study of the shape of these collapsed objects at low enough temperatures [34, 56]. We follow the description of Theodorou and Suter [63] to define the asphericity and acylindricity of a multi-block copolymer chain. First, we define the gyration tensor as

$$\mathbf{S} = \frac{1}{N_\xi} \sum_{i=1}^{N_\xi} \mathbf{s}_i \mathbf{s}_i^T = \overline{\mathbf{ss}^T} = \begin{bmatrix} \overline{x^2} & \overline{xy} & \overline{xz} \\ \overline{xy} & \overline{y^2} & \overline{yz} \\ \overline{xz} & \overline{yz} & \overline{z^2} \end{bmatrix}, \quad (16)$$

where $\mathbf{s}_i = \text{col}(x_i, y_i, z_i)$ is the position vector of each bead, which is considered with respect to the center of mass of the beads $\sum_{i=1}^{N_\xi} \mathbf{s}_i = 0$, and the over-bars denote an average over all beads N_ξ . When the gyration tensor of the whole chain is considered, then $N_\xi = nN$. For the blocks $N_\xi = N$, the gyration tensor and relevant properties are calculated for each block separately and then an average over all blocks is taken,

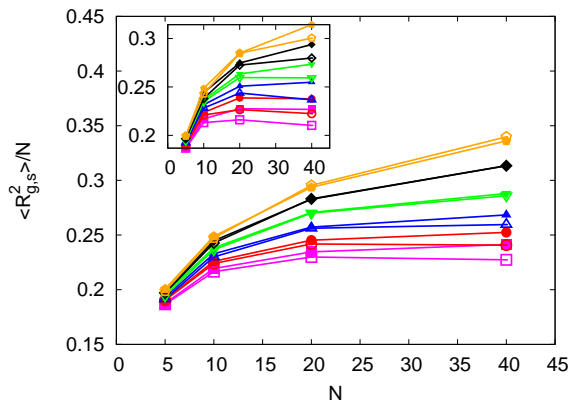


Figure 7. (Color online) Mean-square gyration radius as a function of the side-chain length N . Full symbols correspond to $N_b = 50$, whereas open symbols to $N_b = 100$. Data for different temperatures are shown, starting from below $T = 1.5$, up to $T = 3.0$. In the main part of the figure $\sigma = 1.0$. The inset illustrates the corresponding data for the case $\sigma = 0.5$.

irrespective of their type. The gyration tensor is symmetric with real eigenvalues and, hence, a cartesian system that this tensor is diagonal can always be found, i.e.,

$$\mathbf{S} = \text{diag}(\overline{X^2}, \overline{Y^2}, \overline{Z^2}), \quad (17)$$

where the axes are also chosen in such a way that the diagonal elements (eigenvalues of \mathbf{S}) $\overline{X^2}$, $\overline{Y^2}$, and $\overline{Z^2}$ are in a descending order ($\overline{X^2} \geq \overline{Y^2} \geq \overline{Z^2}$). These eigenvalues are called the principal moments of the gyration tensor. From the values of the principal moments, one defines quantities such as the asphericity b

$$b = \overline{X^2} - 1/2(\overline{Y^2} + \overline{Z^2}). \quad (18)$$

When the particle distribution is spherically symmetric or has a tetrahedral or higher symmetry, then $b = 0$. The acylindricity c

$$c = \overline{Y^2} - \overline{Z^2} \quad (19)$$

is zero when the particle distribution is in sync with a cylindrical symmetry. Therefore, the acylindricity and asphericity are relevant quantities that would characterize the shape of our bottle-brush polymers. These quantities are taken with respect to S , to the sum of the eigenvalues, i.e. the square gyration radius of the chain, which we have also calculated independently on our original cartesian coordinates, in order to check our results. Henceforth, this quantity will be absorbed in the definition of asphericity and acylindricity and all results will be normalized under this norm.

Assuming an ellipsoidal shape and based on the calculation of the above eigenvalues of the gyration tensor, one can define an effective volume expression [64]

$$V^{eff} = 4\pi\sqrt{3} \prod_{i=1}^3 \sqrt{\lambda_i}, \quad (20)$$

where $\lambda_1 = \overline{X^2}$, $\lambda_2 = \overline{Y^2}$, and $\lambda_3 = \overline{Z^2}$, are the eigenvalues of the radius of gyration tensor. Then, the effective radius of a sphere with the same volume as this ellipsoid

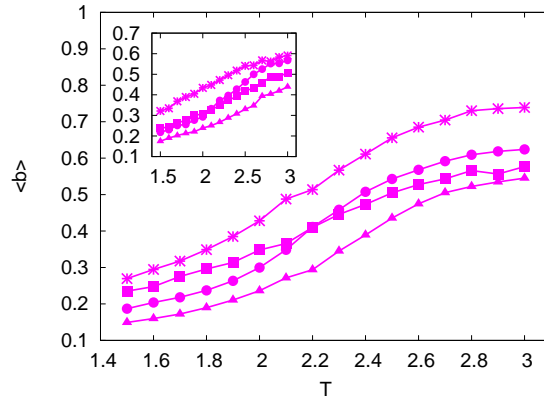


Figure 8. (Color online) Normalized asphericity as a function of the temperature. The main panel shows data for $\sigma = 1.0$, whereas $\sigma = 0.5$ in the inset. The cases $N_b = 50$ and $N = 5$ (stars), $N = 10$ (squares), $N = 20$ (circles), and $N = 40$ (triangles) are shown.

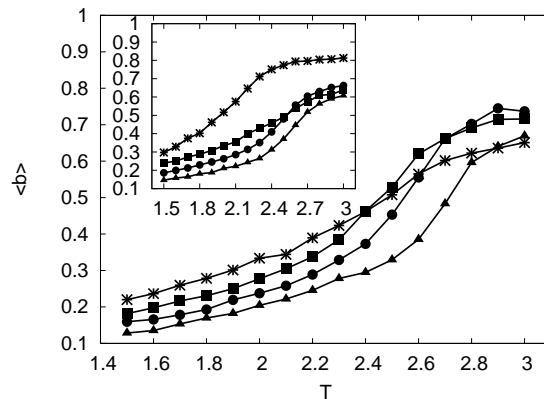


Figure 9. Same as in figure 8, but for $N_b = 100$.

(V^{eff}) is given by the geometrical mean of individual radii $R_g^{eff} = \sqrt[3]{\prod_{i=1}^3 \sqrt[6]{\lambda_i}}$. This can be compared to the volume of an effective sphere defined by the gyration radius $R_g = \sqrt{\sum_{i=1}^3 \lambda_i}$. Such an analysis goes clearly beyond the scope of the present study.

In figure 8 we show results for the asphericity as a function of temperature for macromolecules with backbone length $N_b = 50$. At temperatures below $T = 2.2$, where for all bottle-brush cases collapsed brushes occur, we observe that chains with longer side chains overall adopt a more spherical shape. This means that the increase of the side chains stiffens the backbone is not enough to change the overall picture of the macromolecule, that is a more spherical shape for higher symmetry structure as the side-chain length is increased. The results for backbone length $N_b = 100$ shown in figure 9 illustrate the same behavior. Furthermore, as the temperature increases, there is a significant change in the shape of the bottle brush from a globular coil to an elongated object. Although we can see that we depart from globular structure, we can say very little on whether we obtain a coil-like structure or a homogeneous

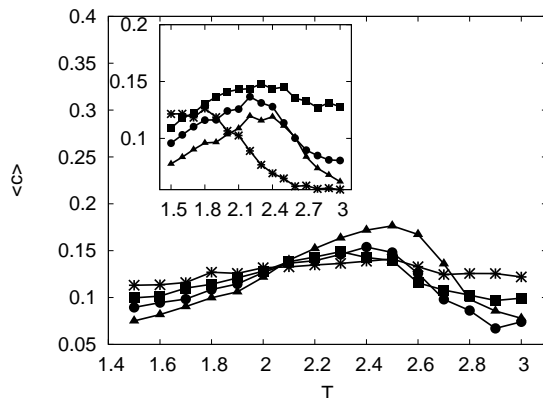


Figure 10. Normalized acylindricity as a function of the temperature. The main panel's data refer to grafting density $\sigma = 1.0$, whereas those of the inset to $\sigma = 0.5$. $N_b = 100$ in both panels. The cases $N = 5$ (stars), $N = 10$ (squares), $N = 20$ (circles), and $N = 40$ (triangles) are shown.

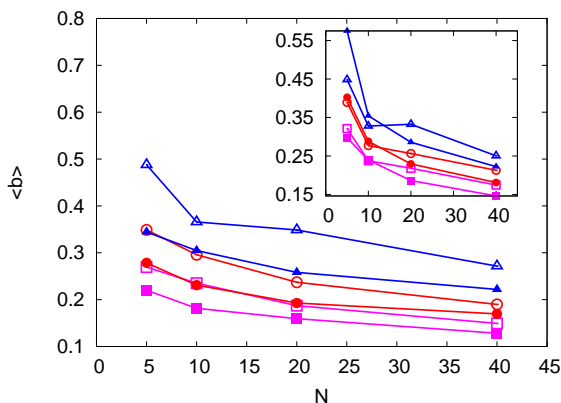


Figure 11. (Color online) Normalized asphericity as a function of the side-chain length N for $\sigma = 1.0$ and $\sigma = 0.5$ (inset). Open symbols refer to $N_b = 50$, whereas full symbols to $N_b = 100$. Different temperatures are shown $T = 1.5$ (squares), $T = 1.8$ (circles), and $T = 2.1$ (triangles).

bottle brush similar to a collapsed brush with a rigid backbone [29] from this quantity. Furthermore, it is worth noting (figure 10) that such non spherical objects possess a cylindrical symmetry, even at low temperatures, and this cylindrical symmetry is only distorted at intermediate temperatures, i.e., within the crossover regime between collapsed chains (globules) and coils or cylindrical brushes. This effect, albeit weak and with a peak appearing at different temperatures depending on the choice of parameters, is clearly shown in figure 10, where for temperatures in the range $2 < T < 2.6$ $\langle c \rangle$ a shallow maximum is observed. Finally, regarding the dependence of the bottle-brush asphericity on the length of the side chains N in the collapsed state, we can observe in figure 11 that the increase of the side-chain length N favors a more spherical symmetry for the bottle brush, advancing in this way the backbone stiffening.

5. Synopsis

In this study we have discussed the structural properties of single-component bottle-brush polymers under poor solvent conditions. We attempted to give a complete picture of the structural properties of these macromolecules within the feasible range of chain lengths, accessible to our simulations. For our range of parameters, which is also similar to the range appearing in experiments [2, 4, 10, 11, 12, 51], we identified the different configurational states for a bottle-brush polymer under poor solvent conditions. At low temperatures, the bottle-brush chain collapses, forming spherical-like objects with a constant density close to the center of mass of the macromolecule, irrespective of the choice of parameters σ , N_b , and N . Thus, the density profile showed a dependency only on the total number of monomers. For higher temperatures, there is a crossover from such collapsed configurations to coil-like structures or cylindrical brushes depending on the choice of the parameters σ , N_b , and N . For small grafting densities, backbone, and chain lengths, coil-like structures are favored, whereas, as the values of the above properties increase, we smoothly obtain brushes with monomers homogeneously distributed around the backbone, similar to a bottle-brush polymer with a rigid backbone [29].

An interesting aspect regarding the shape of bottle-brush polymers with a flexible backbone is that the increase of the side-chain length overwhelms the stretching of the side chains, which is caused by the steric repulsions between monomers, as the side-chain length increases. For this reason, bottle brushes of smaller N have lower spherical or higher symmetry compared to brushes with higher N , in contrast to what one may naively expect. We also studied the acylindricity of bottle-brush polymers. We found that the macromolecule maintains a highly cylindrical symmetry for all these states. Only within the range of temperatures corresponding to the crossover regime between the globular (collapsed) state and coil/brush regime a weak deviation from this behavior is observed. Overall, our results consist a first attempt towards the study of bottle-brush polymers with a flexible backbone and a first step in order to compare results with the case of two-component bottle-brush polymers with a flexible backbone under poor solvent conditions.

References

- [1] Maleki H and Theodorakis P E 2011 *J. Phys.: Condens. Matter* **23** 505104
- [2] Zhang M and Müller A H E 2005 *J. Polym. Sci.* **43** 3461
- [3] Subbotin A V and Semenov A N 2007 *Polym. Sci.* bf 49 1328
- [4] Sheiko S S, Sumerlin B S and Matyjaszewski K 2008 *Prog. Polym. Sci.* **33** 759
- [5] Potemkin I I and Palyulin V V 2009 *Polym. Sci.* **51** 123
- [6] Binder K and Milchev A 2012 *J. Polym. Sci.* **50** 1515
- [7] Walther A and Müller A H E *Chem. Rev.* 2013 in press
- [8] *Carbon Nanotubes: Science and Applications*, ed. M. Meyyappan, CRC, Boca Raton, 2004
- [9] Thomassin J-M, Molenberg I, Huynen I, Debuigne A, Alexandre M, Jerome C and Detrembleur C 2010 *Chem. Commun.* **46** 3330

- [10] Rathgeber S, Pakula T, Matyjaszewski K and Beers K L 2005 *J. Chem. Phys.* **122** 124904
- [11] Zhang B, Gröhn F, Pedersen J S, Fischer K and Schmidt M 2006 *Macromolecules* **39** 8440
- [12] Hsu H-P, Paul W, Rathgeber S and Binder K 2010 *Macromolecules* **43** 1592
- [13] Hsu H-P, Paul W and Binder K 2010 *Macromolecules* **43** 3094
- [14] Theodorakis P E, Hsu H-P, Paul W and Binder K 2011 *J. Chem. Phys.* **135** 164903
- [15] Feuz L, Strunz P, Geue T, Textor M and Borisov O 2007 *Eur. Phys. J E.* **23** 237
- [16] Lee H I, Matyjaszewski K, Yu-Su S and Sheiko S S 2008 *Macromolecules* **41** 6073
- [17] Knaapilo M, Stepanyan R, Torkkeli M, Garamus V M, Galbrecht F, Nehls B S, Preis E, Scherf U and Monkman A P 2008 *Phys. Rev. E* **77** 051809
- [18] Klein J 2009 *Science* **323** 47
- [19] Shiokawa K, Itoh K and Nemoto M 1999 *J. Chem. Phys.* **111** 8165
- [20] Subbotin A, Saariaho M, Ikkala M and ten Brinke G 2000 *Macromolecules* **33** 3447
- [21] Chang R, Kwak Y and Gebremichael Y 2009 *J. Mol. Biol.* **39** 648
- [22] Elli D, Ganazzoli F, Timoshenko E G, Kuznetsov Y A and Connolly R 2004 *J. Chem. Phys.* **120** 6257
- [23] Connolly R, Bellesia G, Timoshenko E G, Kuznetsov Y A, Elli S and Ganazzoli F 2005 *Macromolecules* **38** 5288
- [24] Yethiraj A 2005 *J. Chem. Phys.* **125** 204901
- [25] Hsu H-P, Paul W and Binder K 2007 *Macromol. Theory Simul.* **16** 660
- [26] Hsu H-P, Paul W and Binder K 2008 *J. Chem. Phys.* **129** 204904
- [27] Sheiko S S, Borisov O V, Prokhorova S A and Möller M 2004 *Eur. Phys. J. E* **13** 125
- [28] Khalatur P G, Shirvanyanz D G, Staravoitova N Y and Khokhlov A R 2000 *Macromol. Theory Simul.* **9** 141
- [29] Theodorakis P E, Paul W and Binder K 2009 *Europhys. Lett.* **88** 63002
- [30] Theodorakis P E, Paul W and Binder K 2010 *J. Chem. Phys.* **133** 104901
- [31] Theodorakis P E, Paul W and Binder K 2011 *Eur. Phys. J. E* **34** 52
- [32] Erukhimovich I, Theodorakis P E, Paul W and Binder K 2011 *J. Chem. Phys.* **134** 054906
- [33] Theodorakis P E, Paul W and Binder K 2010 *Macromolecules* **46** 5137
- [34] Theodorakis P E and Fytas N G 2012 *Am. J. Condens. Matter Phys.* **2** 101
- [35] de Gennes P G 1979 *Scaling Concepts in Polymer Physics* (Cornell University Press: Ithaca)
- [36] Birshtein T M and Zhulina E B 1984 *Polymer* **25** 1453
- [37] Witten T A and Pincus P A 1986 *Macromolecules* **19** 2509
- [38] Birshtein T M, Borisov O V, Zhulina E B, Khokhlov A R and Yurosowa T A 1987 *Polym. Sci. U.S.S.R.* **29** 1293
- [39] Ligoure C and Leibler L 1990 *Macromolecules* **23** 5044
- [40] Ball R C, Marko J F, Milner S T and Witten T A 1991 *Macromolecules* **24** 69
- [41] Rouault Y and Borisov O V 1996 *Macromolecules* **29** 2605
- [42] Saariaho M, Ikkala O, Szleifer I, Erukhimovich I and ten Brinke G 1997 *J. Chem. Phys.* **107** 3267
- [43] Guillou J C L and Zinn-Justin J 1980 *Phys. Rev. B* **21** 3976
- [44] des Cloizeaux J and Jannink G 1990 *Polymers in Solution, Their Modeling and Structure* (Clarendon: Oxford)
- [45] Schäfer L 1999 *Excluded Volume Effects in Polymer Solutions as Explained by the Renormalization Group* (Springer: Berlin)
- [46] Rabin Y and Bruinsma 1994 *Soft Order in Physical Systems* (Plenum: New York)
- [47] Halperin A and Zhulina E B 1991 *Europhys. Lett.* **15** 417
- [48] Grest G S and Kremer K 1986 *Phys. Rev. A* **33** 3628
- [49] Murat M and Grest G S 1989 *Macromolecules* **22** 4054
- [50] Binder K 1995 *Monte Carlo and Molecular Dynamics Simulations in Polymer Science* (Oxford University Press: New York)
- [51] Lecommandoux S, Chilecot F, Borsali R, Schappacher M, Deffieux A, Brulet A and Cotton J P 2002 *Macromolecules* **35** 8878

- [52] Grest G S and Murat M 1993 *Macromolecules* **26** 3108
- [53] Theodorakis P E and Fytas N G 2011 *Soft Matter* **7** 1038
- [54] Theodorakis P E and Fytas N G 2011 *Europhys. Lett.* **93** 43001
- [55] Fytas N G and Theodorakis 2011 *J. Phys.: Condens. Matter* **23** 235106
- [56] Theodorakis P E and Fytas N G 2012 *J. Chem. Phys.* **136** 094902
- [57] Murat M and Grest G S 1991 *Macromolecules* **24** 704
- [58] Berendsen H J C, van der Spoel D and van Drunen R 1995 *Comp. Phys. Comm.* **19** 43
- [59] Lindahl E, Hess B and van der Spoel D 2001 *Mol. Mod.* **7** 306
- [60] van Gunsteren W F and Berendsen H J C 1988 *Mol. Simul.* **1** 173
- [61] Shirvanyants D, Panyukov S, Liao S and Rubinstein M 2008 *Macromolecules* **41** 1475
- [62] Beckrich P, Johner A, Semenov A N, Obukhov S P, Benoit H and Wittmer J P 2007 *Macromolecules* **40** 3805
- [63] Theodorou D N and Suter U W 1985 *Macromolecules* **18** 1206
- [64] Hadizadeh S, Linhananta A and Plotkin S S 2011 *Macromolecules* **44** 6182